Available online at www.sciencedirect.com
SCIENCE DIRECT
Polymer 47 (2006) 1820–1829
polymer
www.elsevier.com/locate/polymer

Highly efficient electroluminescent biphenylyl-substituted poly(*p*-phenylenevinylene)s through fine tuning the polymer structure

Chun Huang [a,b], Chang-Gua Zhen [a], Siew Ping Su [a], Chellappan Vijila [a], Bavani Balakrisnan [a], Mark Dai Joong Auch [a], Kian Ping Loh [b], Zhi-Kuan Chen [a,*]

[a] *Institute of Materials Research and Engineering, 3 Research Link, Singapore 117602*
[b] *Department of Chemistry, National University of Singapore, Singapore 119260*

Received 4 May 2005; received in revised form 16 January 2006; accepted 19 January 2006
Available online 7 February 2006

Abstract

A series of novel biphenylyl-substituted PPV derivatives, polymers **1–4**, with different substitution patterns, has been synthesized and characterized. These polymers possess excellent solubilities, good thermal stabilities, and high-photoluminescent efficiencies. ^{1}H NMR measurements indicated that the polymers contain negligible tolane-bisbenzyl (TBB) structural defects. Light-emitting diodes fabricated from the four polymers with the configuration of ITO/PEDOT:PSS (50 nm)/polymer (80 nm)/LiF (0.4 nm)/Ca (20 nm)/Ag emitted a saturated green light and demonstrated maximum current efficiencies of 5.1, 4.5, 4.7, and 1.4 cd/A for polymers **1–4**, respectively. The much higher current efficiencies of polymers **1–3** than polymer **4** are ascribed to more balanced charge transport in the polymer layers of the three polymers, which has been confirmed by time of flight (TOF) charge mobility measurement. The hole mobilities of the polymers at the applied electric field of 2.0×10^5 V/cm are 4.70×10^{-6}, 3.83×10^{-6}, 7.21×10^{-6}, and 1.76×10^{-5} cm^2/Vs for polymers **1–4**. This research indicated that fine tuning the substitution pattern of the polymer side chains is an effective way to optimize the LED device performance by controlling the structural defects as well as balancing the charge mobility of the polymers.

Keywords: Light-emitting diodes; Poly(*p*-phenylenevinylene); Electroluminescent efficiency

1. Introduction

Poly(*p*-phenylenevinylene) and its derivatives (PPVs) have been intensely investigated as electroluminescent polymers for polymer light emitting diodes (PLEDs) in the past decade due to their high-photoluminescent efficiency, good thermal stability and mechanical property, and facile structural modification to tailor the optical/electronic properties [1–12]. However, two major issues still remained in PPV-based polymers, which could retard their success in PLEDs application. The first issue is the structural defects in the polymers. The major structural defects in PPVs prepared through the Gilch method are tolane-bisbenzyl (TBB) moieties, which are formed due to irregular linkages during the polymer chain propagation. It has been demonstrated that these structural defects could decrease the device operational lifetime as well as the electroluminescent (EL) efficiency [7]. There are two possible ways that can be utilized to solve this problem. The first is to make use of the electronic effect of side chains on the monomers to guide the polymer chain propagation so as to reduce the proportion of the irregular linkages in the polymers [7,13]. The second approach is developed by our group through using steric hindrance effect of the side chains on the monomers, which is even more effective than the electronic effect to suppress the TBB structural defects in PPVs [14,15]. However, the electroluminescent efficiency of the polymers reported in our previous work need be further improved. The unsatisfactory EL efficiency of the reported polymers may be due to the second issue: imbalance of charge transport in the polymer layer. Hence, more research effort on further development of the materials is needed to realize devices with higher EL efficiency through balancing the charge transport property.

In this paper, we report the synthesis of a series of novel biphenylyl-substituted PPV derivatives and their materials and device characterizations. The design of the PPVs, with a biphenylyl side group with two long branched alkoxy side chains which aid in control of the structural defects and enable

* Corresponding author. Tel.: +65 6874 4331; fax: +65 6872 0785.
E-mail address: zk-chen@imre.a-star.edu.sg (Z.-K. Chen).

0032-3861/$ - see front matter © 2006 Elsevier Ltd. All rights reserved.
doi:10.1016/j.polymer.2006.01.069

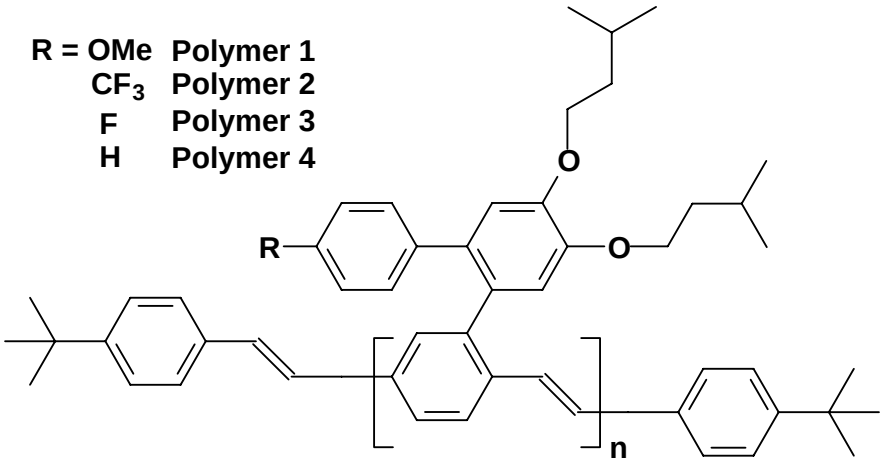

Fig. 1. Chemical structures of biphenylyl-substituted PPV derivatives.

good solubility, has already been reported in our earlier work [15]. In this report, we have introduced another side group such as electron donating (methoxy group) or electron withdrawing group (trifluoromethyl or fluoro group) on the second phenyl ring of the biphenylyl group at the *para*-position. These groups theoretically could affect the energy levels of the polymers and thus their charge transport properties. The secondary effect of these side groups is that they can further reduce the backbone/backbone interaction if there is any in the parent structure [16]. Polymers **1**–**3** have different substitution patterns such as methoxy, trifluoromethyl, fluorine groups, respectively, and polymer **4**, which is the parent structure, has been synthesized for comparison. It is found that the EL efficiency can be largely improved by introducing these small groups into the biphenylyl side groups (Fig. 1).

2. Experimental section

Nuclear magnetic resonance (NMR) spectra were collected on a Bruker ACF 400 spectrometer using chloroform-*d* as a solvent and tetramethylsilane (TMS) as an internal standard. EI mass spectra were obtained from a Micromass VG7035F mass spectrometer. Elemental analysis was performed on a Perkin Elmer 2400 elemental analyzer for C and H determinations. Ultraviolet–visible (UV–vis) and fluorescence spectra were obtained using a Shimadzu UV 3101PC UV–vis–NIR spectrophotometer and a Perkin Elmer LS 50B luminescence spectrometer, respectively. The relative PL quantum yield of the polymers in chloroform solution was determined using quinine sulfate (1×10^{-5} M dissolved in 0.1 M H_2SO_4) as a reference. The absolute PL quantum yields of the polymer films were determined using an integrating sphere (Lab Sphere Com) with He–Cd laser (325 nm, 11 mW) as an excitation source. Cyclic voltammetry (CV) experiments were conducted at room temperature on an AUTOLAB PGSTST30 under argon atmosphere. All potentials were measured in a three-electrode cell with 0.10 M tetrabutylammonium hexafluorophosphate (Bu_4NPF_6) in acetonitrile as the electrolyte, using a Ag/AgCl electrode (3 M KCl) as the reference electrode (−0.04 V vs. SCE). All experimental values were corrected with respect to SCE. GPC was conducted on a Waters 2690 separation module equipped with a Waters 2410 differential refractometer HPLC system and Waters Styragel HR3, HR4 and HR5 columns in series using polystyrene as a standard and HPLC grade THF as the eluent. DSC was run on a DSC 2920 module in conjunction with a TA instrument system. A heating rate of 20 °C/min from −50 to 280 °C and a nitrogen flow rate of 50 cm^3/min were employed. Thermogravimetric analysis (TGA) was conducted on a TA instrument system with a TGA 2050 thermogravimetric analyzer under a heating rate of 20 °C/min from 25 to 800 °C and a nitrogen flow rate of 120 cm^3/min.

3. LED device fabrication

The polymers were dissolved in toluene and filtered through a 0.2 μm PTFE filter for device fabrication. Patterned indium tin oxide (ITO) coated glass substrates were cleaned with acetone, isopropanol and distilled water sequentially in ultrasonic bath. The cleaned substrates were treated with oxygen plasma and spin-coated with 50 nm of poly(3,4-ethylenedioxythiophene) (PEDOT) doped with poly(styrene-sulfonic acid) (PSS), followed by drying in 120 °C for 15 min. The polymer solutions were spin-coated to form an active layer with a thickness of about 80 nm and transferred into a chamber under vacuum of 1×10^{-6} Torr. A 0.4 nm LiF was deposited onto the surface of the active layer to help electron injection, and then 20 nm Ca and 150 nm Ag were deposited sequentially to form the cathode. The current–voltage, current–luminance characteristics were determined in a dry box with a Keithley 2420 source meter and with a calibrated photodiode. EL spectra were recorded with an Ocean Optics USB2000 miniature fiber optic spectrometer.

4. Charge mobility measurement

The mobility of charge carriers in these polymers was studied using a conventional time of flight (TOF) photoconductivity technique. A sandwich type device configuration was used for the measurement. The polymer films were prepared on an ITO (sheet resistance of 20 Ω/sq) patterned

glass substrate using a 3 mg/ml concentrated polymer solution prepared in chloroform, using a drop casting method in saturated solvent environment. The film thickness was measured using a surface profiler (KLA-Tencor P10 surface profiler) and found to be in the range of 0.7–1 μm. These films were kept at 60 °C for 3 h in a nitrogen atmosphere to remove the residual solvent. A 60 nm Al electrode was evaporated onto the polymer film under high vacuum condition (10^{-7} Torr). The TOF measurement system was composed of a pulsed Nitrogen (N_2) laser (Oriel 79074), a pulse generator (SRS-DG535), a DC voltage source (Kenwood PWR18-2), and a digital oscilloscope (Agilant–Infiniium, 1 GHz, 4 Gsa/s). The N_2 laser with pulse width <4 ns, pulse energy 90 μJ, and pulse repetition rate of 1 Hz, was shot on the ITO side of the device and the photocurrent, under the influence of applied electric field, was monitored using the oscilloscope. The photocurrent transients were averaged over 25 repetitions of laser shots and the transit times were obtained. The mobilities of the charges were calculated using the relation $\mu = d^2/Vt_{tr}$, where d is the polymer film thickness, V is the applied voltage and t_{tr} is the transit time.

5. Synthesis of the polymers

5.1. Preparation of 1,2-bis(3′-methylbutoxy)benzene (*A*)

A solution of catechol (27.53 g, 0.25 mol) in 100 ml of ethanol was slowly added to a stirred solution of KOH (35.07 g, 0.63 mol) in 350 ml of ethanol at room temperature. The reaction mixture was stirred for 1 h. A solution of 3-methylbutyl bromide (113.25 g, 0.75 mol) in 50 ml of ethanol was added dropwise. The reaction mixture was refluxed overnight. Ethanol was removed by rotary evaporation and the reaction mixture was partitioned between ethyl acetate and sodium carbonate solution. After drying over sodium sulfate, the product was obtained by reduced pressure distillation to get 38.2 g 1,2-bis(3′-methylbutoxy)benzene (61%). ^{1}H NMR (ppm) (400 MHz, $CDCl_3$): δ 6.914 (s, 4H), 4.059–4.025 (t, 4H), 1.895–1.861 (m, 2H), 1.757–1.707 (m, 4H), 0.993–0.976 (m, 12H).

5.2. Preparation of 4,5-bis(3′-methylbutoxy)-1, 2-dibromobenzene (*B*)

A solution of bromine (15.3 g, 96 mmol) in 100 ml of glacial acetic acid was added to a solution of 1,2-bis(3′-methylbutoxy)benzene (10.00 g, 40 mmol) in 300 ml of a mixture of methanol and chloroform at 0 °C. The reaction mixture was stirred for 5 h, after which it was basified by addition to sodium carbonate (10%, 2 l) and extracted with dichloromethane (3×500 ml). The combined organic layers were washed with water (200 ml×2) and dried over anhydrous sodium sulfate. Then the solvent was removed on a rotary evaporator, the residue was purified by flash column with the mixture of hexane and CH_2Cl_2 (8:1) to offer 15.67 g 4,5-bis(3′-methylbutoxy)-1,2-dibromobenzene (yield 96%). ^{1}H NMR (ppm) (400 MHz, $CDCl_3$): δ 7.086 (s, 2H), 4.006–3.973 (t, 4H), 1.864–1.831 (m, 2H), 1.741–1.691(m, 4H), 0.998–0.971 (m, 12H).

5.3. Preparation of 2-(4′,5′-bis(3″-methylbutoxy)-2′-bromo)-phenyl-p-xylene (*C*)

In an argon flushed two neck round-bottom flask, a mixture of *p*-xylene boronic acid (4.8 g, 30 mmol), 12.24 g (30 mmol) of 4,5-bis(3″-methylbutoxy)-1,2-dibromobenzene, 0.15 g tetrakis(triphenylphosphine) palladium, 100 ml of 2 M sodium carbonate and 200 ml of toluene were stirred at 80 °C overnight. After cooling down, it was extracted with ethyl acetate and washed with brine and dried over magnesium sulfate. The solvent was removed on a rotary evaporator, the residue was purified by column eluted with hexane and CH_2Cl_2 (8:1) to offer 11.04 g of 2-(4′,5′-bis(3″-methylbutoxy)-2′-bromo)phenyl-*p*-xylene (yield 85%). ^{1}H NMR (ppm) (400 MHz, $CDCl_3$): δ 7.186–7.131 (m, 3H), 6.979 (s, 1H), 6.747 (s, 1H) 4.081–3.966 (m, 4H), 2.372 (s, 3H), 2.111 (s, 3H), 1.914–1.710 (m, 6H), 1.023–0.962(m, 12H).

5.4. Preparation of 2-(4′,5′-bis(3″-methylbutoxy)-2′-bromo)-phenyl-α,α′-diacetoxy-p-xylene (*D*)

2-(4′,5′-Bis(3″-methylbutoxy)-2′-bromo)phenyl-*p*-xylene (0.86 g, 2 mmol), *N*-bromosuccinimide (0.72 g, 4 mmol) and AIBN (20 mg) in benzene (5 ml) was heated at reflux for 2 h. After cooling down, the solvent was removed and the mixture was partitioned between ethyl acetate and water. The organic layer was dried over Na_2SO_4 and the solvent was removed to give a brown oil containing a mixture of brominated products. A mixture of the crude residue and anhydrous potassium acetate (4 g) in glacial acetic acid (8 ml) was heated at reflux overnight. After cooling, the mixture was partitioned between dichloromethane and water. The organic layer was dried over Na_2SO_4 and the solvent was removed to give a brown oil (1.11 g) containing a mixture of acetylated products. The crude product was purified by column eluted with hexane and CH_2Cl_2 (6:1) to offer 0.46 g of 2-(4′,5′-bis(3″-methylbutoxy)-2′-bromo)phenyl-α,α′-diacetoxy-*p*-xylene (yield 42%). ^{1}H NMR (ppm) (400 MHz, $CDCl_3$): δ 7.508 (d, $J=8.0$, 1H), 7.419 (d, $J=8.0$, 1H), 7.215 (s, 1H), 7.118 (s, 1H), 6.786 (s, 1H), 5.161 (s, 2H), 5.032 (d, $J=12.6$, 1H), 4.884 (d, $J=12.6$, 1H), 4.079 (t, 2H), 3.996–3.955 (m, 2H), 2.135 (s, 3H), 2.042 (s, 2H), 1.911–1.611 (m, 6H), 1.285–0.904 (m, 12H).

5.5. Preparation of 2-(4′,5′-bis(3″-methylbutoxy)-2′-p-methoxyphenyl)-phenyl-α,α′-diacetoxy-p-xylene (*E1*)

In an argon flushed two neck round-bottom flask, a mixture of 4 mmol of *p*-methoxyphenyl boronic acid, 1.1 g (2 mmol) of 2-(4′,5′-bis(3″-methylbutoxy)-2′-bromo)phenyl-α,α′-diacetoxy-*p*-xylene, 50 mg tetrakis(triphenylphosphine), 10 ml 2 M sodium carbonate and 150 ml of toluene were stirred at 90 °C overnight. After cooling down, it was extracted with ethyl acetate and washed with brine and dried with magnesium sulfate. Then the solvent was removed on a rotary evaporator,

the residue was purified by column eluted with hexane and CH_2Cl_2 (1:1) to offer a colorless oil (1.10 g, yield 95%). ^1H NMR (ppm) (400 MHz, $CDCl_3$): δ 7.296–7.262 (m, 4H), 7.163 (s, 1H), 7.007 (d, $J=8.0$, 2H), 6.942(s, 1H), 6.831(s, 1H), 6.721(d, $J=8.0$, 2H), 5.072 (m, 2H), 4.792 (d, 1H), 4.715 (d, 1H), 4.122–4.038 (m, 4H), 3.761 (s, 3H), 2.088 (s, 3H), 2.068 (s, 3H), 1.782–1.742 (m, 6H), 1.014–0.980 (m, 12H).

E2, **E3**, **E4** were synthesized, purified and characterized in a similar manner as that for **E1**.

*5.6. Preparation of 2-(4′,5′-bis(3″-methylbutoxy)-2′-p-trifluoromethylphenyl)phenyl-α,α′-diacetoxy-p-xylene (**E2**)*

Yield 90%. ^1H NMR (ppm) (400 MHz, $CDCl_3$): δ 7.439 (d, $J=8.0$, 2H), 7.330 (d, 1H), 7.284 (s, 1H), 7.219 (d, $J=8.0$, 2H), 7.110(s, 1H), 6.954(s, 1H), 6.82(s, 2H), 5.039 (m, 2H), 4.830 (d, 1H), 4.779(d, 1H), 4.130–4.062 (m, 4H), 2.061 (s, 3H), 1.968 (s, 3H), 1.900–1.753 (m, 6H), 1.020–0.986 (t, 12H).

*5.7. Preparation of 2-(4′,5′-bis(3″-methylbutoxy)-2′-p-fluorophenyl)phenyl-α,α′-diacetoxy-p-xylene (**E3**)*

Yield 90%. ^1H NMR (ppm) (400 MHz, $CDCl_3$): δ 7.329–7.271 (m, 2H), 7.118 (s, 1H), 7.059–7.024 (m, 2H), 6.931 (s, 1H), 6.882–6.838 (m, 1H), 5.054 (m, 2H), 4.802 (d, 1H), 4.751 (d, 1H), 4.125–4.039 (m, 4H), 2.083 (s, 3H), 1.980 (s, 3H), 1.891–1.745 (m, 6H), 1.018–0.981 (m, 12H).

*5.8. Preparation of 2-(4′,5′-bis(3″-methylbutoxy)-2′-phenyl)-phenyl-α,α′-diacetoxy-p-xylene (**E4**)*

Yield 90%. ^1H NMR (ppm) (400 MHz, $CDCl_3$): δ 7.284–7.252 (m, 2H), 7.153 (s, 4H), 7.088 (s, 2H), 6.974 (s, 1H), 6.850 (s,1H), 5.054 (m, 2H), 4.802 (d, 1H), 4.734 (d, 1H), 4.110–4.060 (m, 4H), 2.080 (s, 3H), 1.972 (s, 3H), 1.886–1.767 (m, 6H), 0.998 (m, 12H).

*5.9. Preparation of 2-(4′,5′-bis(3″-methylbutoxy)-2′-p-methoxyphenyl)phenyl-α,α′-dihydroxy-p-xylene (**F1**)*

A solution of 2.0 mmol of compound 2-(4′,5′-bis(3″-methylbutoxy)-2′-*p*-methoxy-phenyl)phenyl-α,α′-diacetoxy-*p*-xylene in 10 ml THF was dropwise added to a 100 ml round-bottom flask with 0.2 g of lithium aluminum hydrate and 60 ml of THF and stirred for 1 h, then the reaction was quenched by added saturated sodium sulfate solution slowly until white solid come out. The solid was filtered off and the filtrate was washed with water and brine, dried with sodium sulfate. After the solvent was removed, 0.98 g of white solid product was obtained (yield 100%), which was used for next step synthesis without further purification.

F2, **F3**, **F4** were synthesized and purified in a similar manner as that for **F1**.

*5.10. Preparation of 2-(4′,5′-bis(3″-methylbutoxy)-2′-p-methoxy-phenyl)phenyl-α,α′-dichloro-p-xylene (**M1**)*

In a 10 ml round-bottom flask, 2.0 mmol of 2-(4′,5′-bis(3″-methylbutoxy)-2′-*p*-methoxy-phenyl)phenyl-α,α′-dihydroxy-*p*-xylene and 5 ml of thionyl chloride was stirred at 50 °C for 3 h. On completion of reaction, the mixture was poured into ice water and partitioned between ethyl acetate and water. The organic layer was dried over Na_2SO_4 and the solvent was removed to give a brown oil. The residue was purified by column chromatography using hexane:methylene chloride (5:1) as the eluent to yield 0.49 g of colourless solid (46%). MS: *m/z* 528.2, ^1H NMR (ppm) (400 MHz, $CDCl_3$): δ 7.423 (d, 1H), 7.301 (d, 1H), 7.161 (s, 1H), 6.980 (s, 1H), 6.958 (s, 2H), 6.918 (s, 1H), 6.721 (d, 2H), 4.526 (m, 2H), 4.363 (d, 1H), 4.219 (d, 1H) 4.113–4.070 (m, 4H), 3.746 (s, 3H), 1.906–1.752 (m, 6H), 1.018–0.981 (t, 12H). ^{13}C NMR (PPM) (400 MHz, $CDCl_3$) 149.2, 148.3, 142.0, 137.5, 136.1, 133.7, 133.5, 132.0, 130.9, 130.7, 130.2, 127.9, 116.4, 115.7, 113.8, 68.2, 55.6, 46.1, 44.3, 38.5, 38.4, 25.6, 23,1. Anal. Calcd for $C_{31}H_{38}Cl_2O_3$: C, 70.31, H, 7.23. Found: C, 70.55; H, 7.03.

M2, **M3**, **M4** were synthesized, purified and characterized in a similar manner as that for **M1**.

*5.11. Preparation of 2-(4′,5′-bis(3″-methylbutoxy)-2′-p-trifluoromethyl-phenyl)phenyl-α,α′-dichloro-p-xylene (**M2**)*

Yield 42%. MS: *m/z* 566.1, ^1H NMR (ppm) (400 MHz, $CDCl_3$): δ 7.446–7.421 (m, 3H), 7.319–7.296 (m, 1H), 7.189 (d, 2H), 7.084 (s, 1H), 6.973 (d, 2H), 4.501–4.424 (m, 2H), 4.395–4.305 (m, 2H), 4.142–4.087 (m, 4H), 1.929–1.747 (m, 6H), 1.024–0.987 (t, 12H). ^{13}C NMR (PPM) (400 MHz, $CDCl_3$) 149.3, 149.1, 144.8, 141.3, 137.8, 136.0, 132.5, 132.2, 131.1, 130.5, 130.2, 128.3, 125.3, 123.2, 116.2, 115.7, 68.3, 68.2, 45.8, 44.2, 38.4, 38.3, 23.6, 23.0. Anal. Calcd for $C_{31}H_{35}Cl_2F_3O_2$: C, 65.61, H, 6.22. Found: C, 65.21; H, 5.96.

*5.12. Preparation of 2-(4′,5′-bis(3″-methylbutoxy)-2′-p-fluorophenyl)phenyl-α,α′-dichloro-p-xylene (**M3**)*

Yield 60%. MS: *m/z* 516.1, ^1H NMR (ppm) (400 MHz, $CDCl_3$): δ 7.432 (d, 1H), 7.309 (d, 1H), 7.116 (s, 1H), 7.036–7.001 (t, 2H) 6.949–6.933 (d, 2H), 6.884–6.841 (t, 2H), 4.535 (m, 2H), 4.371 (d, 1H), 4.282 (d, 1H) 4.138–4.076 (m, 4H), 1.930–1.756 (m, 6H), 1.024–0.985 (t, 12H). ^{13}C NMR (PPM) (400 MHz, $CDCl_3$) 149.3, 148.6, 137.6, 137.1, 136.0, 133.0, 132.0, 131.5, 130.8, 130.4, 128.1, 116.3, 115.7, 115.3, 115.1, 68.3, 68.2, 46.0, 44.2, 38.5, 38.4, 25.6, 23.1, 23.0. Anal. Calcd for $C_{30}H_{35}Cl_2FO_2$: C, 69.63, H, 6.82. Found: C, 60.00; H, 6.51.

*5.13. Preparation of 2-(4′,5′-bis(3″-methylbutoxy)-2′-phenyl)-phenyl-α,α′-dichloro-p-xylene (**M4**)*

Yield 60%. MS: *m/z* 498.1, ^1H NMR (ppm) (400 MHz, $CDCl_3$): δ 7.417 (d, 1H), 7.303 (d, 1H), 7.174–7.145 (m, 4H), 7.067–7.048 (t, 2H) 6.994 (s, 1H), 6.947 (s, 1H), 4.501 (m, 2H),

4.386 (d, 1H), 4.357 (d, 1H) 4.142–4.084 (m, 4H), 1.912–1.743 (m, 6H), 1.023–0.988 (t, 12H). ^{13}C NMR (PPM) (400 MHz, $CDCl_3$) 149.3, 148.6, 141.8, 141.1, 137.5, 136.1, 134.1, 132.1, 130.7, 130.4, 130.0, 129.3, 128.9, 128.3, 128.0, 126.8, 116.4, 115.8, 68.3, 46.0, 44.3, 38.5, 38.4, 25.6, 23.1. Anal. Calcd for $C_{30}H_{35}Cl_2O_2$: C, 72.13, H, 7.26. Found: C, 72.16; H, 7.36.

*5.14. Preparation of poly[2-(2′-p-methoxyphenyl-4′,5′-bis(3″-methylbutoxy))phenyl-1,4-phenylene vinylene] (polymer **1**)*

A solution of 2-(4′,5′-bis(3″-methylbutoxy)-2′-*p*-methoxyphenyl)phenyl-α,α′-dichloro-*p*-xylene (0.8 mmol) in 15 ml of anhydrous THF was added a solution of 0.48 ml 1 M of potassium *tert*-butoxide in 8 ml of anhydrous THF at room temperature with stirring for 24 h, after which 0.1 g of 4-(*tert*-butyl)benzyl chloride in 2 ml of THF was added in one portion. After stirred for another 6 h. The mixture was added into methanol and the resulting yellow precipitate was collected by filtration. The polymer was dissolved in toluene and reprecipitated from a mixture solvent of methanol and water (*V*:*V*=7:1) for three times. The collected polymer was extracted through Soxhlet extractor using methanol followed by acetone. 0.182 g of bright yellow polymer was obtained with a yield of 50%. ^{1}H NMR (ppm) (400 MHz, $CDCl_3$): δ 7.50–6.662 (11H), 4.114–4.075 (4H), 3.719 (3H), 1.895–1.770 (6H), 1.017–0.966 (12H).

Polymers **2**–**4** were synthesized, purified and characterized in a similar manner as that for polymer **1**.

*5.15. Preparation of poly[2-(2′-p-trifluoromethyl-phenyl-4′,5′-bis(3″-methylbutoxy))phenyl-1,4-phenylene vinylene] (polymer **2**)*

Yield 41%. ^{1}H NMR (ppm) (400 MHz, $CDCl_3$): δ 7.383–6.950 (11H), 4.118 (4H), 1.899–1.791 (6H), 1.022–0.981 (12H).

*5.16. Preparation of poly[2-(2′-p-fluorophenyl-4′,5′-bis(3″-methylbutoxy))phenyl-1,4-phenylene vinylene] (polymer **3**)*

Yield 51%. ^{1}H NMR (ppm) (400 MHz, $CDCl_3$): δ 7.500–6.964 (11H), 4.135 (4H), 1.890–1.791 (6H), 1.021–0.975 (12H).

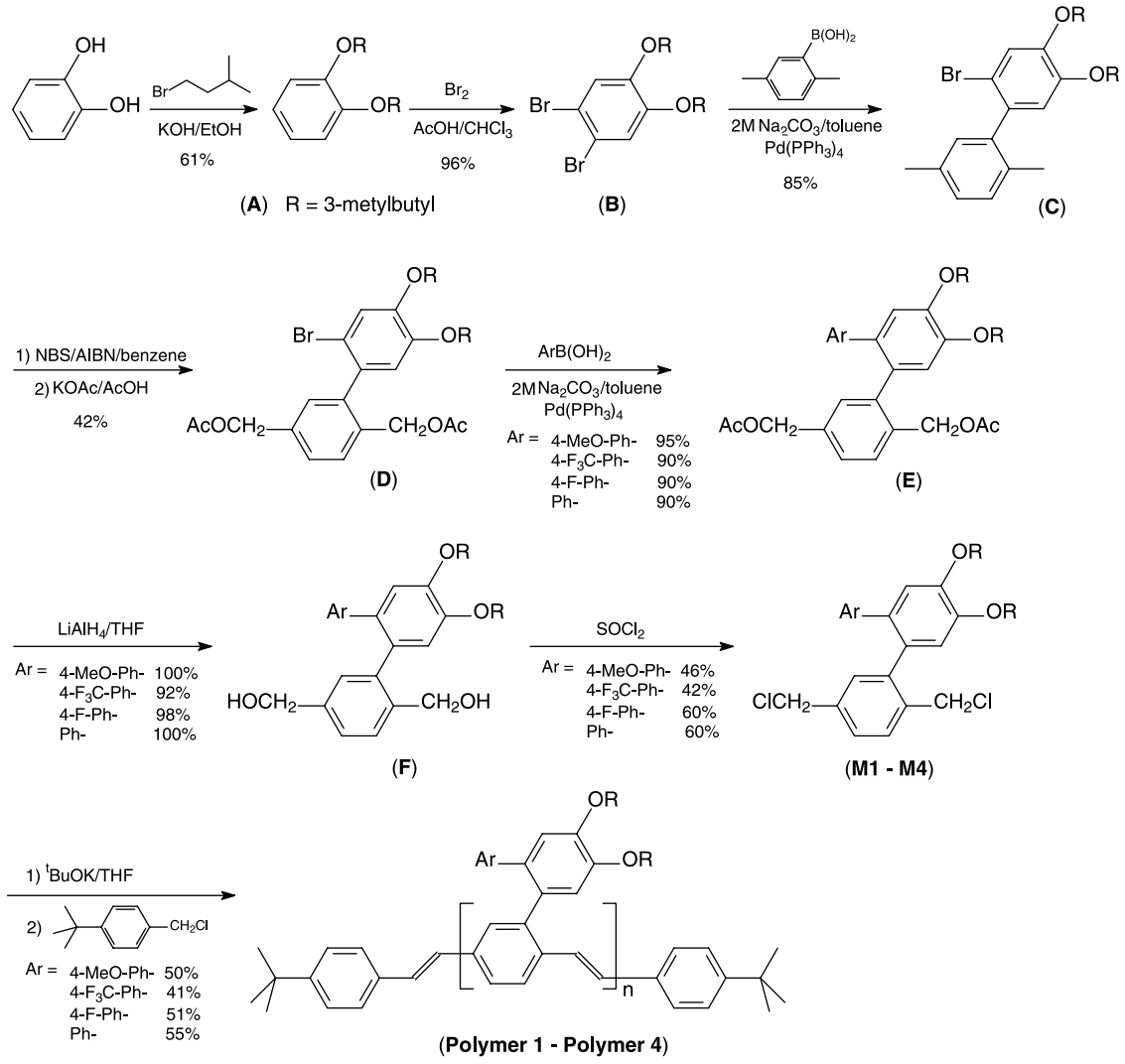

Scheme 1. Synthesis of the biphenylyl-substituted PPV derivatives.

*5.17. Preparation of poly[2-(2′-phenyl-4′,5′-bis(2″-methylbutoxy))phenyl-1,4-phenylene vinylene] (polymer **4**)*

Yield 55%. ^{1}H NMR (ppm) (400 MHz, $CDCl_3$): δ 7.500–6.801 (12H), 4.180 (4H), 1.890–1,791 (6H), 1.018–0.975 (12H).

6. Result and discussion

6.1. Synthesis and characterization

The PPV polymers were obtained with satisfactory yields following the synthetic routes outlined in Scheme 1. During the synthesis of the monomers, bromination by NBS is a key step and it can be conducted in two ways. Route I is to carry out the bromination of compound C using NBS initiated by AIBN, then converting the bromomethyl groups to acetoxyl methyl groups (Compound D). Compound D is reacted further with excess aryl boronic acid to form compound E with the desired biphenylyl side groups. Route II is to convert the bromo group on compound C to aryl group through the Suzuki reaction to form the biphenylyl side groups. Then NBS bromination is conducted followed by esterification to get compound E. It is worthwhile to note that the bromination through route II may cause undesirable bromo substitution reaction on the biphenylyl group, especially when the second aryl ring contains electron donating group. This brominated by-product is very difficult to be removed by normal column purification. It is well established that a small amount of bromine atoms on the polymers will remarkably decrease the EL efficiency of the device. Therefore, we chose route I to prepare compound D first and then form the biphenylyl groups by the Suzuki coupling reaction with excess aryl boronic acid compounds to ensure that there are no bromine atoms remained on the products. The Gilch polymerization method was used to carry out the polymerization to achieve high molecular weight polymers. ^{1}H NMR spectroscopy was used to measure the content of tolane-bisbenzyl (TBB) structural defects in the polymers. The ^{1}H NMR spectrum of polymer **1**, as an example, is shown in Fig. 2. The signal at 7.2–7.5 and 6.4–7.1 ppm are assigned to protons of vinylene groups and phenyl/phenylene groups, respectively. The peaks at 3.7 and 4.1 ppm are due to the resonance of $-OCH_3$ and $-OCH_2-$, respectively. No signal in the range of 2.4–2.8 ppm is observed, which indicates that there are negligible TBB structural defects on the polymer chains of polymer **1**. No TBB defects also could be detected in polymers **3** and **4**. However, it was found that there are about 1.0% TBB defects on the polymer chains of polymer **2**. Although the monomer M2 possesses the highest steric hindrance effect among the monomers for the polymerization, the observation of a small amount of TBB defects in polymer **2** implies that strong electron-withdrawing group on the side chain will cause irregular linkages during the polymerization because of the electronic effect (Table 1).

The thermal stability of the polymers has been investigated by TGA under nitrogen. The TGA traces of the polymers are shown in Fig. 3. The onset of decomposition temperatures of the polymers was found to be 378, 345, 347 and 330 °C for polymers **1**–**4**, and weight loss of 5% occurred at 429, 405, 407 and 399 °C, respectively. It can be found that incorporation of an addition side group on the biphenyl group can improve the thermal stability of the polymers by 15–30 °C. The glass transition temperature of the polymers has been measured by differential scanning calorimetry (DSC) at a heating rate of 20 °C/min under flowing nitrogen. No obvious T_g was observed for the polymers except for polymer **4**, which showed a T_g at 164 °C. The DSC trace of polymer **4** was shown in Fig. 3 as an insert.

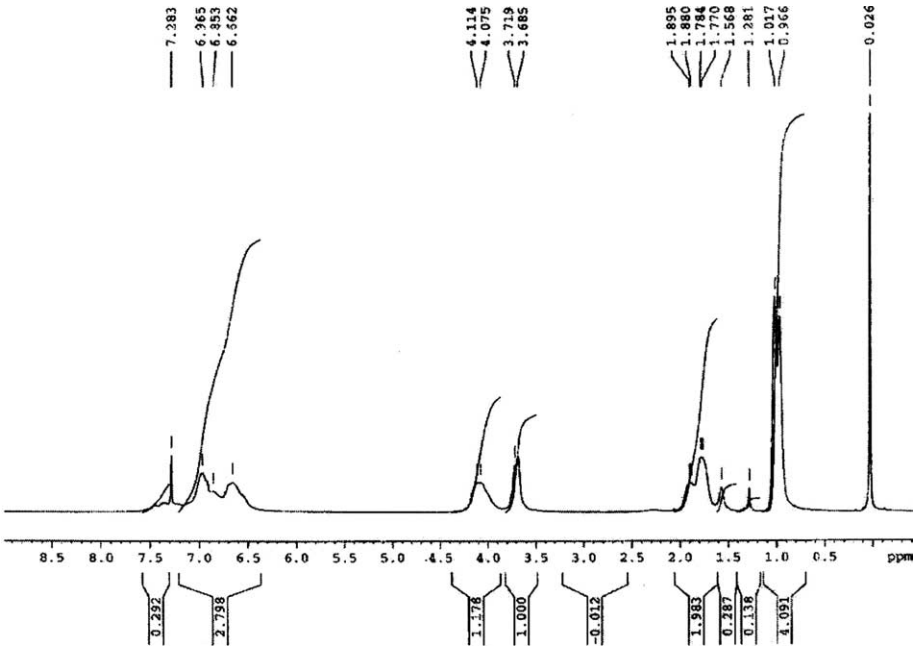

Fig. 2. ^{1}H NMR spectrum of polymer **1** in $CDCl_3$.

Table 1
Physical properties of the polymers

Polymers	M_n/M_w ($\times 10^4$)	PDI	T_d (°C) (onset)	T_g (°C)	TBB defects
Polymer **1**	6.4/24	3.75	378	–	Negligible
Polymer **2**	8.2/31	3.78	345	–	About 1%
Polymer **3**	17/65	3.82	347	–	Negligible
Polymer **4**	11/41	3.72	330	164	Negligible

6.2. Optical and electrochemical properties

The absorption and photoluminescence (PL) spectra of the polymers in $CHCl_3$ solutions were measured at room temperature. As shown in Fig. 4, the polymers demonstrated very similar UV absorption and PL emission spectra because of their similar chemical structures. The π–π^* band gap of the polymers were estimated from the absorption edge, and found to be 2.54 eV for all the four polymers. The relative fluorescence quantum efficiencies (η_{PL}) of the polymers in chloroform were determined to be 66, 44, 69 and 64% for polymers **1**–**4**, respectively, using quinine sulfate (1×10^{-5} M dissolved in 0.1 M H_2SO_4) as a reference. The η_{PL} of polymer **2** is lower than the other three polymers in solutions, which may be connected with the extent of conformational freedom of the strong electron withdrawing trifluoromethyl groups on the side chains which enhances the non-radiative decay processes. The absolute PL quantum yields of the polymer films were measured using an integrating sphere and found to be 54, 52, 50, and 45% for polymers **1**–**4**, respectively. The η_{PL} in solid state is only slightly lower than that in solution indicates that the additional non-radiative decay channels in solid state are very few. The higher η_{PL} of the first three polymers than that of polymer **4** indicated that incorporation of an additional side group on the biphenylyl group could further reduce the non-radiative decay channels due to lowering the inter-chain interaction in solid state. The enhanced η_{PL} of polymer **2** in solid state than that in solution may be ascribed to the exciton confinement effect of the polymer in solid state due to the bulky side groups and the rigid polymer backbone. It has been reported that PL quantum efficiency could be higher when the effective conjugation length is in the same range as the exciton confinement length [17].

Cyclic voltammetry (CV) was employed to investigate the electrochemical behaviors of the polymers. The polymer films deposited on Pt electrodes were scanned positively in 0.10 M tetrabutylammonium hexafluorophosphate (Bu_4NPF_6) acetonitrile solution. The onset potentials for oxidation were observed at 0.98, 1.19, 1.12, and 1.07 V (vs SCE) for polymers **1**–**4**, respectively. The HOMO energy levels were estimated to be −5.38, −5.59, −5.52, and −5.47 eV for the four polymers according to the equation [18] HOMO $= -([E_{onset}]^{ox} + 4.4)$ eV. The respective LUMO energy levels were estimated to be −2.84, −3.05, −2.98, and −2.93 eV, by combining the HOMO energy with band gap obtained from the optical method. Although different substituents on the biphenylyl group does not result in obvious changes in changing

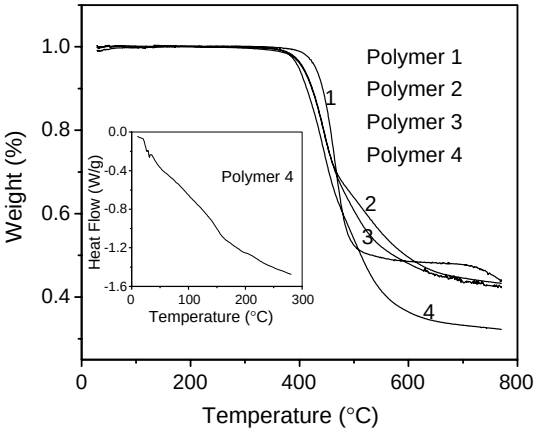

Fig. 3. Thermalgravimetric analysis of polymers **1**–**4** in nitrogen at a heating rate of 20 °C/min. The insert shows the DSC scan for polymer **4** in flowing nitrogen at a heating rate of 20 °C/min.

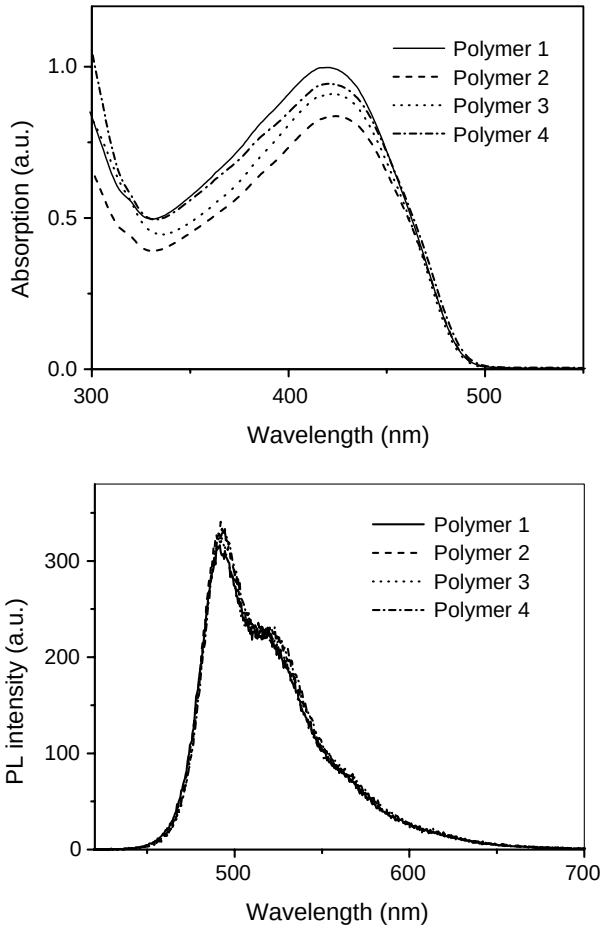

Fig. 4. UV–vis absorption and PL spectra (excited at 420 nm) of the polymers in chloroform solutions ($\sim10^{-6}$ M).

Table 2
Optical and electrochemical data of the polymers

Polymers	UV λ_{max} (nm) in $CHCl_3$	Bandgap (eV)	PL λ_{max} (nm) in $CHCl_3$	η_{PL} in $CHCl_3$ (%)	η_{PL} in Film (%)	p-Doping (V)		Energy levels (eV)	
						E_{onset}	E_a	HOMO	LUMO
Polymer **1**	420	2.54	494 524	66	54	0.98	1.49	−5.38	−2.84
Polymer **2**	423	2.54	492 523	44	52	1.19	1.64	−5.59	−3.05
Polymer **3**	424	2.54	492 523	69	50	1.12	1.81	−5.52	−2.98
Polymer **4**	419	2.54	492 524	64	45	1.07	1.65	−5.47	−2.93

the energy band gaps of the polymers, electron donating groups such as methoxy group can elevate both the HOMO and LUMO energy levels by 0.1 eV compared with polymer **4**; while electron withdrawing trifluoromethyl group move the two energy levels down by about 0.1 eV compared with the same reference polymer. This result indicated the polymer energy levels could be tuned even through a remote substituent with different electronic property. The stronger the electron donating (withdrawing) property of the substituents, the greater will be the increase (decrease) in the HOMO (LUMO) energy levels (Table 2).

6.3. Electroluminescent properties of LED devices

LED devices based on the four PPV polymers with the configuration of ITO/PEDOT:PSS (50 nm)/polymer (80 nm)/LiF (0.4 nm)/Ca (20 nm)/Ag (150 nm) were fabricated. The electroluminescence spectra are shown in Fig. 5, in which, all the polymers exhibit similar traces as their PL spectra, with a main peak at around 505 nm and a clear side peak at 540 nm.

The current–voltage (*I–V*) and luminance–voltage (*L–V*) curves of the devices are displayed in Fig. 6. With an increase of the forward bias, both the current and luminance increase simultaneously. The turn-on voltages of the devices are about 3.2–3.5 V for the four polymers. Polymer **4** shows the lowest turn on current and highest current density among the four polymers. On the contrary, it demonstrates the lowest luminance compared to others. The maximum brightness for polymers **1**–**4** is 2694, 1144, 1438, and 450 cd/m^2 at 10 V, respectively. The highest current density but lowest luminance of polymer **4** among the four polymers is an indication of imbalance of the charge transport in the polymer layer in the device and the holes migrate too fast to be fully captured by the electrons injected from the cathode.

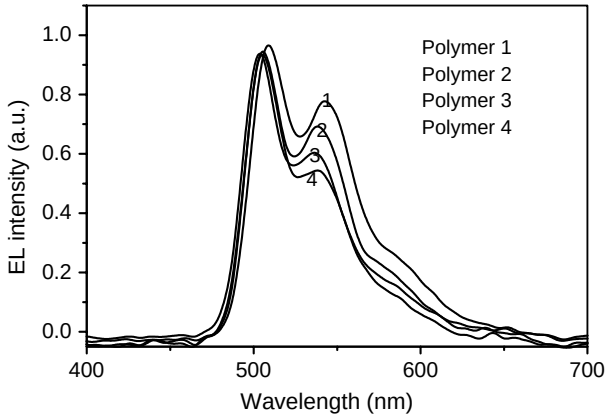

Fig. 5. Electroluminescence spectra of the polymers in the devices of ITO/PEDOT:PSS (50 nm)/polymer (80 nm)/LiF (0.4 nm)/Ca (20 nm)/Ag (150 nm).

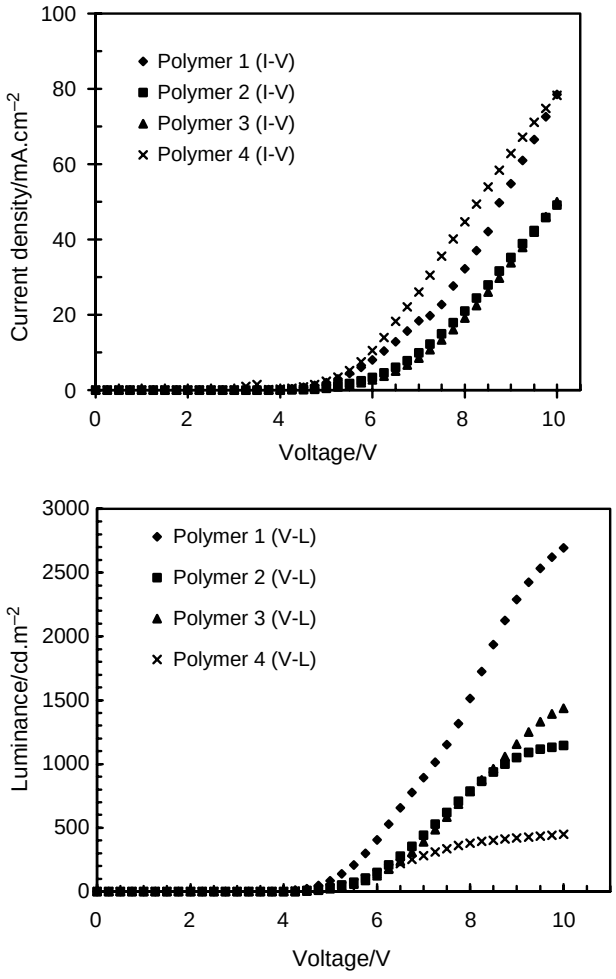

Fig. 6. Current–voltage and luminance-voltage curves of the polymer light-emitting diodes.

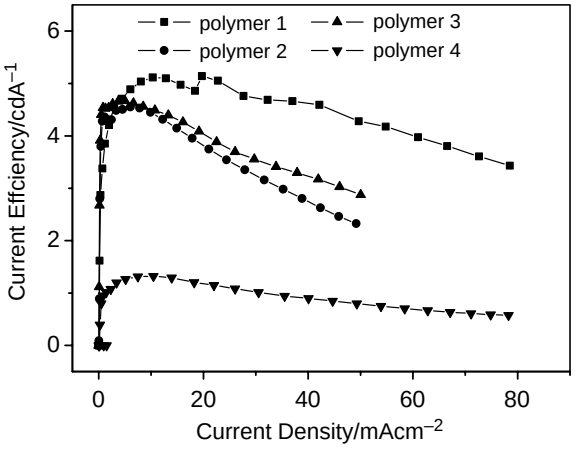

Fig. 7. Dependence of current efficiency of the polymer light-emitting diodes on current density.

As shown in Fig. 7, the maximum current efficiencies of the devices are 5.1, 4.5, 4.7, and 1.4 cd/A for polymers **1**–**4**, which are corresponding to the external quantum efficiencies of 1.33, 1.19, 1.29 and 0.35%, respectively. The quantum efficiency of 0.35% for polymer **4** is comparable to the device efficiency (0.2–0.4%) reported in our previous work based on a very similar polymer [15]. In comparison with polymer **4**, the efficiencies of other three polymers have been improved by two to three times. The performance of 1.19–1.33% of quantum efficiency or 4.5–5.1 cd/A of current efficiency is among the best results reported for PPV-based PLEDs although the devices have not been optimized. In fact, the performance is better than those of PPVs with electron-withdrawing groups, which are developed based on a different strategy to balance the hole-electron transport property by enhancing the electron affinity of the polymers [9,19–21].

In order to confirm the mechanism for the difference of the EL efficiency between polymer **4** and the others, the charge mobility of these polymers was measured using a conventional time of flight (TOF) photoconductivity technique. The typical TOF photocurrent transient for the holes in the drop casted polymer **2** film is shown in Fig. 8 and the shape of the curve indicates the non-dispersive nature of hole transport.

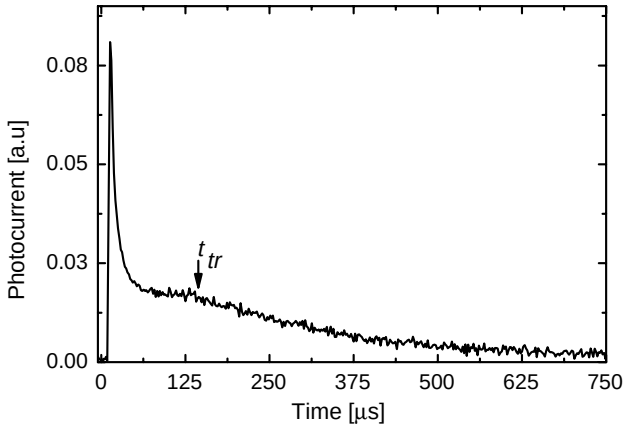

Fig. 8. A typical room temperature TOF holes transient in polymer **2** film for an applied field of 2.0×10^5 V/cm, sample thickness 1.5 μm.

The electron transients showed dispersive behaviors and the exact transit time and reliable electron mobility could not be obtained [22]. The hole mobilities of the polymers were found to be 4.70×10^{-6}, 3.83×10^{-6}, 7.21×10^{-6} and 1.76×10^{-5} cm^2/Vs for polymers **1**–**4** at the applied electric field of 2×10^5 V/cm. The hole mobility of the first three polymers is quite similar, while, that of polymer **4** is much higher than the others. The charge mobility results indicate that the enhanced EL efficiency of the devices of polymers **1**–**3** is due to the success of lowering the hole mobility of the polymers, which balances the hole and electron charges transport in the polymer layer. The highest hole mobility of polymer **4** is also in good agreement with the observation of the highest current density in the *I*–*V* curves of the devices, which is illustrated in Fig. 6. The reduced hole mobility of the polymers by addition of small side groups to the biphenylyl group of polymer **4** could be ascribed to the increase of the hopping distance of charges in the three polymers compared to polymer **4** [23]. The order of the hole mobilities of the polymers follow the sequence of the size of the additional substituents on the biphenylyl groups (reduced from –H, to –F, then to $-OCH_3$, and finally to $-CF_3$), which implies that charge mobility can be easily controlled through tuning the size of the side groups of the polymers.

7. Conclusion

A series of novel biphenylyl-substituted PPV derivatives has been successfully synthesized using the Gilch method. The polymers possess desirable properties such as excellent solubility, high-PL efficiency, good thermal stability, and extremely low-structural defects in the polymer main chains. LED devices with configuration of ITO/PEDOT:PSS (50 nm)/polymer (80 nm)/LiF (0.4 nm)/Ca (20 nm)/Ag (150 nm) revealed that the EL efficiency of polymer **4** can be largely improved by incorporating small groups to the side chains of biphenylyl groups, which can effectively balance the holes and electrons transport in the polymer layer. The lowered hole mobility may be ascribed to the increased hole hopping distance between polymer chains. The results indicated that lowering the hole mobility of PPVs by incorporating bulky side groups could be an alternative effective strategy to balance the charge transport besides enhancing the electron affinity of the polymers.

Acknowledgements

We acknowledge Dr. Zhang Xinghai, Mr. Patrick W. S. Lau, and Ms Tang Shih Ju for their assistance in OLED device fabrication and EL spectra measurement.

References

[1] Burroughes JH, Bradley DDC, Brown AR, Marks RN, Mackay K, Friend RH, et al. Nature (London) 1990;347:539.
[2] Gustafsson G, Cao Y, Treacy GM, Klavetter F, Colaneri N, Heeger AJ. Nature (London) 1992;357:477.

[3] Burn PL, Holmes AB, Kraft A, Bradley DDC, Brown AR, Friend RH, et al. Nature (London) 1992;356:47.
[4] Greenham NC, Moratti SC, Bradley DDC, Friend RH, Burn PL, Holmes AB. Nature (London) 1993;365:628.
[5] Cao Y, Parker ID, Yu G, Zhang C, Heeger AJ. Nature (London) 1999;397: 414.
[6] Segura JL, Martin N. J Mater Chem 2000;10:2403.
[7] Becker H, Spreitzer H, Kreuder W, Kluge E, Schenk H, Parker I, et al. Adv Mater 2000;12:42.
[8] Chen ZK, Meng H, Lai YH, Huang W. Macromolecules 1999;32:4351.
[9] Lee YZ, Chen XW, Chen SA, Wei PK, Fann WS. J Am Chem Soc 2001; 123:2296.
[10] Kim K, Hong YR, Lee SW, Jin JI, Park Y, Sohn BH, et al. J Mater Chem 2001;11:3023.
[11] Jin SH, Kim MY, Kim JY, Lee K, Gal YS. J Am Chem Soc 2004;126:2474.
[12] Liao L, Pang Y, Ding L, Karasz FE. Macromolecules 2004;37:3970.
[13] Johansson DM, Wang XJ, Johansson T, Inganas O, Yu G, Srdanov G, et al. Macromolecules 2002;35:4997.
[14] Chen ZK, Huang W, Wang LH, Kang ET, Chen BJ, Lee CS, et al. Macromolecules 2000;33:9015.
[15] Chen ZK, Lee NHS, Huang W, Xu YS, Cao Y. Macromolecules 2003;36: 1009.
[16] Li AK, Yang SS, Jean WY, Hsu CS, Hsieh BR. Chem Mater 2000;12: 2741.
[17] Manoj AG, Narayan KS, Gowri R, Ramakrishnan S. Synth Met 1999;101: 255.
[18] Cervini R, Li XC, Spencer GWC, Holmes AB, Moratti SC, Friend RH. Synth Met 1997;84:359.
[19] Ko SW, Jung BJ, Ahn T, Shim HK. Macromolecules 2002;35:6217.
[20] Jin Y, Kim J, Lee S, Kim JY, Park SH, Lee K, et al. Macromolecules 2004;37:6711.
[21] Ding L, Egbe DAM, Karasz FE. Macromolecules 2004;37:6124.
[22] Obrzut J, Obrzut MJ, Karasz FE. Synth Met 1989;29:103.
[23] Greenham NC, Friend RH. Semiconductor devices physics of conjugated polymers. In: Ehrenreich H, Spaepen F, editors. Solid state physics, vol. 49. New York: Academic Press, Inc.; 1995. p. 1–149.